Delayed feedback control of periodic orbits without torsion in nonautonomous chaotic systems: Theory and experiment

A. Tamaševičius,[1] G. Mykolaitis,[1,2] V. Pyragas,[1] and K. Pyragas[1,3]
[1]*Semiconductor Physics Institute, A. Goštauto 11, LT-01108 Vilnius, Lithuania*
[2]*Department of Physics, Vilnius Gediminas Technical University, LT-10223 Vilnius, Lithuania*
[3]*Department of Theoretical Physics, Faculty of Physics, Vilnius University, LT-10222 Vilnius, Lithuania*
(Received 13 February 2007; revised manuscript received 4 June 2007; published 6 August 2007)

We demonstrate theoretically and experimentally that the unstable delayed feedback controller is an efficient tool for stabilizing torsion-free unstable periodic orbits in nonautonomous chaotic systems. To improve the global control performance we introduce a two-step control algorithm. The problem of a linear stability of the system under delayed feedback control is treated analytically. Theoretical results are confirmed by electronic circuit experiments for a forced double-well oscillator.

DOI: 10.1103/PhysRevE.76.026203 PACS number(s): 05.45.Gg, 02.30.Ks, 07.05.Dz

I. INTRODUCTION

Control of complex and chaotic behavior has been one of the most rapidly developing topics in applied nonlinear science for more than a decade [1–4]. Many methods have been devised for stabilizing unstable periodic orbits (UPOs) embedded in a chaotic attractor. The delayed feedback control (DFC) method introduced by one of us (K.P.) [5] and later extended by different authors [6–9] has become very popular. The method is noninvasive in the sense that the control signal vanishes when the stabilization of the target orbit is attained. Although the method can be relatively simply implemented in experiments, its theory is rather difficult, since the time-delay dynamics takes place in infinite-dimensional phase spaces. Successful implementations of the method include quite diverse experimental systems from different fields of science (cf. [10] for a review). However, a topological limitation has been pointed out, which means the inability to stabilize periodic orbits without torsion [11] or, more precisely, orbits with an odd number of real Floquet multipliers greater than unity [12,13]. Although it has been recently demonstrated that such a limitation does not generally apply to autonomous systems [14], for nonautonomous systems it remains a crucial factor.

To overcome the odd number limitation an idea of the unstable controller has been proposed [15]. By including an additional unstable mode into the control loop one artificially enlarges the set of real multipliers greater than unity to an even number. So far, this idea has been exploited solely for autonomous systems. A corresponding analytical theory has been developed close to a subcritical Hopf bifurcation [16], and the basins of attraction have been analyzed for different forms of the control force [17].

Due to complexity of the DFC theory, most investigations are restricted to a linear stability analysis and no systematic treatment of global properties, such as the size of basins of attraction, is available in the literature. The importance of such global features has been emphasized even in the original paper [5]. It has been shown that limiting the size of the control force by a simple cutoff increases the domain of attraction of the target state. A more pronounced analysis of the global properties of the DFC has been performed only recently [17–20].

Here we address the concept of the unstable delayed feedback controller to nonautonomous chaotic systems from both theoretical and experimental points of view. We develop an approximate analytical approach for a linear stability analysis of the controlled system and show that the basin of attraction of the stabilized target state can be enlarged via a two-step control algorithm.

II. THEORETICAL CONSIDERATIONS

As a paradigmatic model of nonautonomous chaotic systems let us consider the forced double-well oscillator. If x and y denote the dynamical variables of the oscillator, A is the amplitude, and ω is the frequency of the driving force, then the equations of motion subjected to delayed feedback control read

$$\dot{x} = y, \tag{1a}$$

$$\dot{y} = \alpha x - \gamma x^3 - \beta y + A\cos(\omega t) - k(S + W), \tag{1b}$$

$$\dot{W} = \lambda_c W + kbS, \tag{1c}$$

$$S(t) = x(t) - (1 - R)B(t - \tau), \tag{1d}$$

$$B(t) = x(t) + RB(t - \tau), \tag{1e}$$

where $\alpha > 0$ and $\gamma > 0$ are the parameters of the double-well potential and $\beta > 0$ is the damping parameter. Here we use the extended version [6] of the DFC described by the variables $S(t)$ and $B(t)$ with the delay time $\tau = 2\pi/\omega$ equal to the period of the driving force and the memory parameter $0 < R < 1$. Note that the quantity $B(t)$ can be excluded from Eqs. (1d) and (1e) by writing $S(t) = x(t) - x(t-\tau) + RS(t-\tau)$, but the latter equation contains two delayed variables $x(t-\tau)$ and $S(t-\tau)$. The form (1d) and (1e) with two variables $B(t)$ and $S(t)$ is more convenient from experimental point of view since it requires only one delay line for variable $B(t)$. To overcome the odd number limitation an unstable mode governed by the variable W with the parameter $\lambda_c > 0$ is incorporated. The strength of the feedback force is

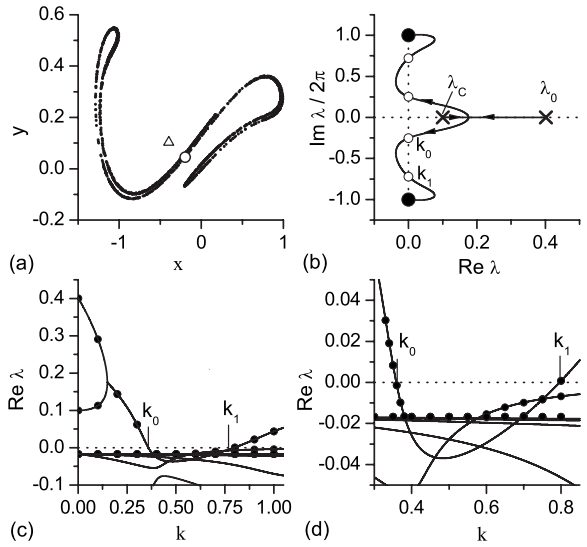

FIG. 1. (a) Stroboscopic map of the forced double-well oscillator for $\alpha=\beta=\gamma=0.3$, $\omega=1$, and $A=0.27$. The open circle marks the target torsion-free UPO. The triangle shows the stable extraneous periodic orbit generated in the first step of control at $C=0$ and $k=0.5$. (b) Root loci of Eq. (7) for $b=0.2$, $R=0.9$, and $\lambda_c=0.1$ as k varies from 0 to ∞. Crosses and black dots show the location of roots for $k=0$ and $k=\infty$, respectively. (c) Real parts of the leading Floquet exponents vs k. Solid lines are solutions of the quasipolynomial, Eq. (7), and dots show the solutions of the exact equation (4). (d) Enlarged essential part of (c).

defined by the parameters b and k. The τ-periodic solutions $x(t)=x_P(t)=x_P(t-\tau)$ of the uncontrolled oscillator (1a) and (1b) are also the solutions of the whole closed loop system (1), since they make zero the control perturbation. Indeed, for such solutions Eqs. (1c)–(1e) are satisfied at $B(t)=x_P(t)/(1-R)$, $S(t)=0$, and $W(t)=0$.

For a certain choice of parameters, the free ($k=0$) oscillator (1a) and (1b) exhibits chaotic behavior. An example of the stroboscopic map for $\alpha=0.3$, $\beta=0.3$, $\gamma=0.3$, $\omega=1.0$, and $A=0.27$ is shown in Fig. 1(a). The symmetric UPO marked by the circle is torsion free; its largest Floquet exponent is $\lambda_0\approx 0.401$ or Floquet multiplier $\mu_0=e^{\lambda_0\tau}\approx 12.423$. The latter value indicates that the orbit is highly unstable. This UPO is the subject of testing our control algorithm. It is interesting to note that the UPO is weakly nonlinear, although it is embedded in the chaotic attractor for which the nonlinearity is an essential factor. By a weakly nonlinear orbit we mean that the influence of the nonlinear term γx^3 on its solution is small and it can be found by perturbation theory. In a zero approximation ($\gamma=0$) the solution for this UPO is

$$x_P^{(0)}(t) = -A\,\mathrm{Re}[e^{i\omega t}/(\omega^2+\alpha-i\omega\beta)]. \tag{2}$$

This approximation is good if $\gamma(x_P^{(0)})^2 \ll \alpha$—i.e., when

$$\gamma A^2/[(\omega^2+\alpha)^2+\omega^2\beta^2] \ll \alpha. \tag{3}$$

The set of parameters chosen above meets this inequality.

If the condition (3) is satisfied, the Floquet exponents of the controlled UPO can be also obtained via a perturbation theory. To present the theory in a general form we introduce vector notation. Let $z=(xyW)^T$ be the vector of the dynamical variables of the system (1) and $z_P=(x_Py_P0)^T$ be the corresponding UPO. Small deviations from the UPO, $\delta z=z-z_P$, may be decomposed into eigenfunctions according to the Floquet theory, $\delta z=e^{\lambda t}u(t)$ and $u(t)=u(t-\tau)$, where λ is the Floquet exponent. The equation for the periodic function $u(t)$ is

$$\lambda u+\dot{u}=Lu+\gamma N[z_P(t)]u-kK(\lambda)u. \tag{4}$$

The matrices L and N,

$$L=\begin{pmatrix}0 & 1 & 0\\ \alpha & -\beta & 0\\ 0 & 0 & \lambda_c\end{pmatrix},\quad N[z_P(t)]=\begin{pmatrix}0 & 0 & 0\\ -3x_P^2(t) & 0 & 0\\ 0 & 0 & 0\end{pmatrix},$$

are, respectively, related to the linear and nonlinear terms of the free system (1), and $K(\lambda)$ is the control matrix:

$$K(\lambda)=\begin{pmatrix}0 & 0 & 0\\ H(\lambda) & 0 & 1\\ -bH(\lambda) & 0 & 0\end{pmatrix},\quad H(\lambda)=\frac{1-e^{-\lambda\tau}}{1-e^{-\lambda\tau}R}.$$

It depends on λ due to the elimination of the delay terms.

We suppose that the target UPO is weakly nonlinear and seek solutions of Eq. (4) in the form of a power series in γ: $\lambda=\lambda^{(0)}+\gamma\lambda^{(1)}+\cdots$, $u=u^{(0)}+\gamma u^{(1)}+\cdots$, and $z_P=z_P^{(0)}+\gamma z_P^{(1)}+\cdots$. In the zero approximation, the right-hand side of Eq. (4) is independent of time and thus $u^{(0)}$ is independent of time as well. Therefore, the zero approximation gives rise to a time-independent eigenvalue problem: $\lambda^{(0)}u^{(0)}=Lu^{(0)}-kK(\lambda^{(0)})u^{(0)}$. If we sought correction terms by the standard perturbation theory, we would come to intricate expressions. We show, however, that the Floquet exponents of the controlled UPO can be derived with accuracy $O(\gamma)$ from a relatively simple time-independent eigenvalue problem. Let us average Eq. (4) over the period of the UPO:

$$\lambda\bar{u}=L\bar{u}+\gamma\overline{N[z_P(t)]u}-kK(\lambda)\bar{u}, \tag{5}$$

where $\bar{\varphi}\equiv(1/\tau)\int_0^\tau\varphi(t)dt$. One can easily verify that this equation can be transformed with accuracy $O(\gamma)$ to

$$\lambda\bar{u}=L\bar{u}+\gamma\overline{N[z_P^{(0)}(t)]}\bar{u}-kK(\lambda)\bar{u}; \tag{6}$$

i.e., if we apply the perturbation theory to Eqs. (5) and (6) we obtain equivalent results up to terms $O(\gamma)$. Equation (6) represents a time-independent eigenvalue problem and leads to a relatively simple quasipolynomial equation

$$\det(L+\gamma\overline{N[z_P^{(0)}(t)]}-kK(\lambda)-I\lambda)=0, \tag{7}$$

where I is the identity matrix.

The mechanism of stabilization is evident from the root loci diagram of Eq. (7) shown in Fig. 1(b). With the increase of k, the positive exponent λ_0 of the uncontrolled UPO, and the eigenvalue λ_c of the unstable mode W approach each other on the real axes, then collide, pass to the complex plane, and move to the stable region $\mathrm{Re}\lambda<0$. For

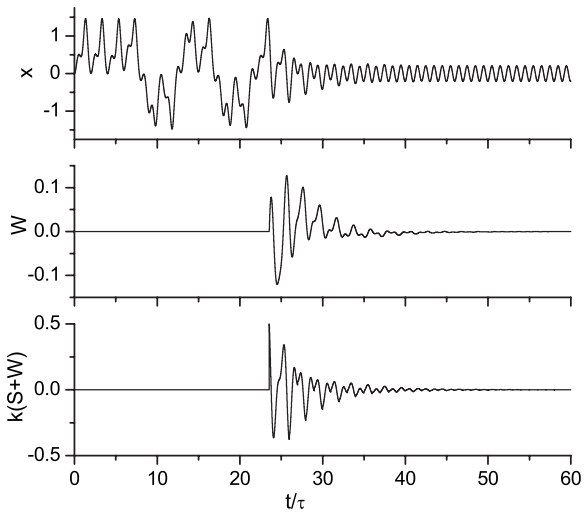

FIG. 2. Successful control of the torsion-free UPO. The results are obtained by numerical solution of Eqs. (1). The control is activated at $t=23.25\tau$; i.e., the control gain $k=0$ for $t<23.25\tau$ and $k=0.5$ for $t\geqslant 23.25\tau$. Other parameters are the same as in Fig. 1.

$k\in[k_0,k_1]\approx[0.359,0.796]$, the target orbit is stable. Figures 1(c) and 1(d) show that the solutions of the quasipolynomial equation (7) are in good quantitative agreement with the values of Floquet exponents obtained numerically from exact equation (4). Note that neglecting the nonlinear term $\gamma N[z_P^{(0)}(t)]$ in Eq. (7) leads only to qualitative but not quantitative agreement with the exact results. Good quantitative results derived from quasipolynomial equation (7) confirm the validity of our analytical approach.

Successful stabilization of the torsion-free UPO is shown in Fig. 2. The results are obtained by numerical solution of the nonlinear delay-differential equations (1). When the system approaches the target orbit the variable W tends to zero and the control perturbation $S+W$ vanishes. Note that the linear stability of the target orbit does not guarantee successful control for any initial conditions. To estimate the basin of attraction we have calculated the statistics of the successful outcomes at different values of k taken from the stability interval $[k_0,k_1]$. The control has been activated from different 1000 points randomly chosen on the chaotic attractor of the free system. By way of illustration, one of numerical experiments for $k=0.38$, 0.54, and 0.7 has shown, respectively, 846, 994, and 992 successful outcomes.

Unfortunately, the current DFC theory cannot give general advice as to how to enlarge the basin of attraction of the stabilized UPO. To improve the global properties usually various limiters are introduced that restrict the size of the control force [5,15,16,19]. Recently it has been shown that the basin of attraction can be enlarged by coupling control forces through the phase of the signal [17]. Here we test an alternative approach based on a two-step algorithm. In our algorithm we do not attempt to reach the target state offhand. In the first step we seek only a rough approach to the desired state. For this aim we detune artificially some of the system parameter. In the second step we return the correct value of the parameter and reach exactly the target state.

The idea of a two-step algorithm is based on the observation that periodic orbits are robust [21]; their form and Floquet multipliers vary slowly with smooth parameter changes. An illustrative example is the period-doubling bifurcation. The UPOs embedded in a chaotic attractor originating from this bifurcation do not differ considerably from stable periodic orbits, which were in the system below the critical value of the chaotic instability. Thus, by switching a proper control parameter in the first step, one can expect a conversion of chaotic motion into a stable periodic motion close to the target UPO (cf. [22]). We refer to this generated periodic motion as an extraneous periodic orbit. In the second step we need only to move the system from the extraneous orbit to the target UPO. Such an algorithm may enlarge the basin of attraction of the target orbit if the extraneous orbit has a larger basin of attraction and if it lies in the basin of attraction of the target orbit. The feasibility of the two-step algorithm is demonstrated in the Appendix by a simple example of the logistic map.

Unfortunately, we do not have a general recommendation for selecting the control parameter which allows us to generate a proper extraneus orbit in the first step of control. For a given system the choice of such a parameter may depend on the convenience of experimental implementation and can be found by trial and error. For the double-well oscillator, we have found that the basin of attraction of the target orbit can be extended by a simple modification of Eq. (1e):

$$B(t)=x(t)+CRB(t-\tau), \tag{8}$$

where C is an auxiliary parameter. When control is off $(k=0)$ we take $C=0$. In the first step, which lasts some time interval t_C, we switch on $k\neq 0$ but hold C at zero. In the second step, we switch on $C=1$. For $t_C=3\tau$, the numerical experiments have shown 100% success rate at any values of $k\in[k_0,k_1]$.

For this system, rigorous consideration of a mechanism of the two-step algorithm is difficult, since one has to deal with the global dynamics in an infinite-dimensional phase space. However, a qualitative explanation of the mechanism is similar to that presented in the Appendix for the simple logistic map. For $C=0$ and $k\neq 0$, the control force does not vanish; it generates an extraneous stable periodic orbit shown in Fig. 1(a) by the triangle. The bifurcation diagram presented in Fig. 3 indicates that the extraneous orbit is linked to the target state by a homotopy; i.e., the two orbits are "continuously connected." The generated orbit is close to the stabilized target UPO [cf. Fig. 1(a)] and lies in its basin of attraction. Numerical analysis shows that the extraneous orbit has better stability properties and larger basin of attraction than those of the stabilized UPO. If $t_C>1/|\lambda_e|$, where λ_e is the leading exponent of the extraneous orbit, then in the first step the phase points located in the larger basin approach the extraneous orbit and in the second step they approach the target orbit.

III. EXPERIMENTAL IMPLEMENTATION

To verify the feasibility of the unstable two-step DFC we have constructed an electronic circuit shown in Fig. 4. The

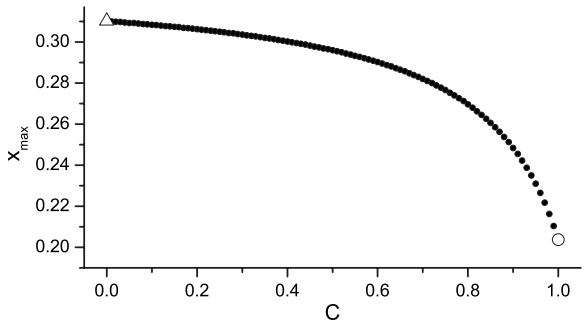

FIG. 3. The maxima of the x variable of delay-differential equations (1) for $k=0.5$ when one changes the parameter C continuously from 1 to 0. The initial value of x_{max} at $C=1$ marked by open circle represents the target state, and the final value at $C=0$ marked by triangle corresponds to the extraneous orbit. Other parameters are the same as in Fig. 1.

OA1-based subcircuit is a double-well nonautonomous oscillator driven by an external sinusoidal oscillator $A\sin(\omega t)$. The LC tank resonance frequency has been set close to the external driving frequency ω. The oscillator is a simplified version of the Young-Silva circuit [23]. The rest of the circuit is a controller. Specifically, the OA2 stage is a buffer, the OA4 stage is an inverter, and the OA7 inverting integrator together with the OA8 inverter plays the role of an unstable unit. The delay unit denoted as a two-terminal box in Fig. 3 is described in details elsewhere [24]. Actually it is a high-order low-pass LCL-type filter. The transfer function of the filter exhibits unity gain and constant delay $\tau=3$ ms in rather wide frequency range, from dc to 3 kHz. Since the upper band limit is higher than the fundamental frequency (333 Hz) and its several higher harmonics of the nonlinear oscillator, the filter can be considered as nearly ideal delay line. Together with the OA5-based adder and the OA6 inverter in the local feedback loop the delay line composes an extended delay subcircuit (the ratio $R15/R14$ is just the parameter R). Eventually, the OA3-based adder via $R3$ completes the feedback loop of the controller. The initial positions of the switches $K1$ and $K3$ are in the closed state as shown in Fig. 4 (this ensures $k=0$ and $W=0$), while the switch $K2$ initially is in the open state (holds $C=0$). All the switches are electronically operated; however, the service circuits are not shown in Fig. 3 for simplicity.

The experimental results are presented in Fig. 5. The left-hand side of the photograph is for the free-running system without control ($k=0$ and $W=0$). The segment of $x(t)$ illustrates typically chaotic behavior of the nonautonomous double-well oscillator. To release the control the switches $K1$ and $K3$ are turned off. At this moment the feedback signal is applied to the oscillator ($k\neq 0$) with the signal $W(t)$ generated by the unstable OA7-OA8 subcircuit. However, in the first step the switch $K2$ is still kept opened, thus holding $C=0$. The second step ($C=1$) is activated by closing $K2$ after a short time t_C, typically of 3–10 ms, which corresponds to a few periods of external force (τ–3τ). After some transients of about 20 ms the double-well chaotic oscillator goes into a stable periodic mode of oscillation, while the signal $W(t)$ and the total control signal $k(S+W)$ vanish as expected.

We emphasize that the two-step control is very important in experiments. When we applied one-step control—i.e., switched $K1$, $K2$, and $K3$ at the same moment—not all of the attempts were successful. Neither the periodic orbit was stabilized nor the system remained chaotic, but the output signals ran away from the attractor to the supply voltage ±15 V. To characterize the performance of the controller quantitatively we built a common threshold circuit, generating a single output pulse for each unsuccessful shot. The pulses were registered by means of a standard counter. The control had been applied to the system at a repetition rate of 5 Hz for 6 h. Thus, more than $N=100\,000$ shots had been performed. The rate of success slightly depended on the parameter R. For example, the numbers of unsuccessful control events were the following: $n=55\,118$ and $n=43\,561$ for $R=0.8$ and $R=0.9$, respectively. Accordingly, the rate of success $(N-n)/N$ was from about 45% to 55% in the case of one-

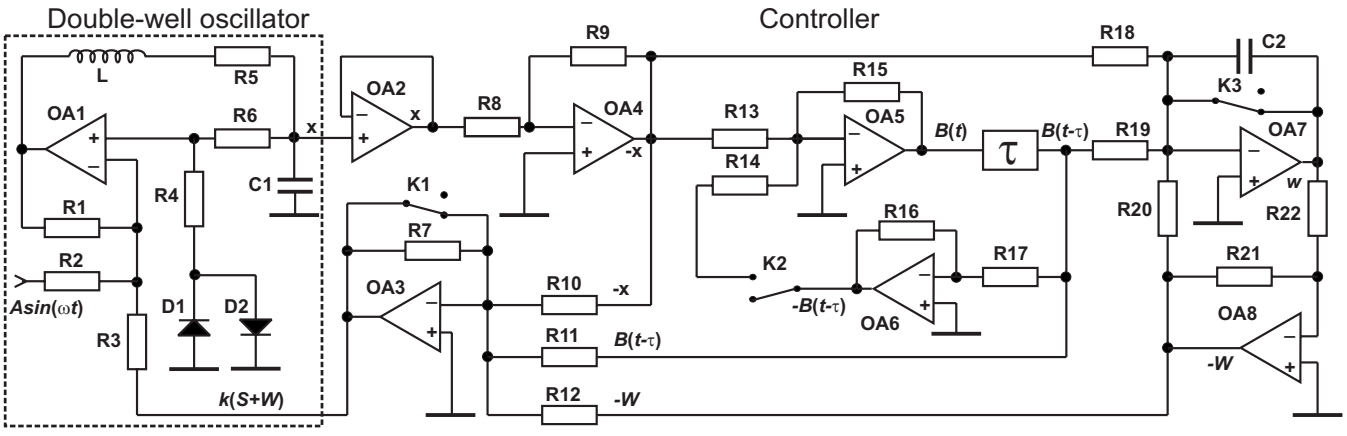

FIG. 4. Circuit diagrams of the double-well oscillator and the delayed feedback controller. The operational amplifiers are low-offset OP07E-type chips; the diodes are general-purpose 1N4148 devices. $L=210$ mH, $C1=1.1\mu$F, $C2=1\mu$F, $R1=1.1$ kΩ, $R2=R3=20$ kΩ, $R4=16$ kΩ, $R5=82$ Ω, $R6=100$ kΩ, $R7=33$ kΩ, $R8=R9=R10=R12=R13=R15=R16=R17=R20=R21=R22=10$ kΩ, $R11=62$ kΩ, $R14=11.9$ kΩ, $R18=8.2$ kΩ, and $R19=51$ kΩ. Delay unit labeled by τ is described in Ref. [24], delay time $\tau=3$ ms. Drive amplitude $A=2.8$ V, frequency $f=\omega/2\pi=333$ Hz.

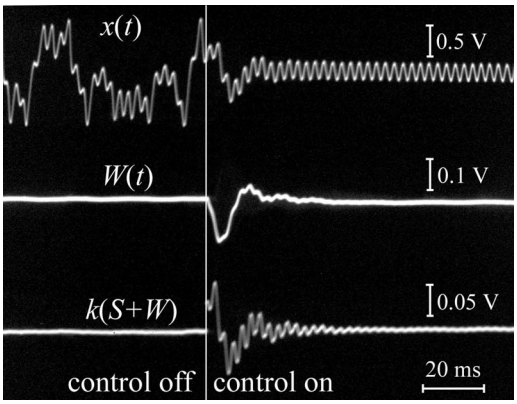

FIG. 5. Experimental snapshots of the output signal of the double-well oscillator $x(t)$, the variable $W(t)$, and the control signal $k(S+W)$. The horizontal and vertical scales are inscribed in the photograph. The fine vertical line indicates the time instant when the first step of control is activated (switches $K1$ and $K3$ are turned off). The second step of control (switch $K2$ is turned on) is activated 3 ms later.

step control. In contrast, the two-step control ensured 100% of success.

IV. CONCLUSION

We have presented theoretical and experimental evidence that the unstable delayed feedback controller is a practical and efficient tool to overcome the odd number limitation in nonautonomous chaotic systems. Our analytical approach is generic for any weakly nonlinear periodic orbits and can be applied to a wider class of nonautonomous oscillators and delayed feedback controllers. We have shown numerically and experimentally that the two-step control algorithm improves the global control performance. The generality of this algorithm requires further investigation but even the present results show that this idea is promising. We have presented an experimental implementation of the unstable controller for a chaotic system. Thus the concept of the unstable feedback loop works very well and widens the applicability of the delayed feedback control techniques to nonautonomous systems without torsion.

APPENDIX: TWO-STEP DELAYED FEEDBACK CONTROL OF THE LOGISTIC MAP

The simplest dynamical toy models to which two-step delayed feedback control can be applied are time discrete maps. They are easier to handle since the dimension of phase space stays finite even if the control loop is included. Thus, visualization of global properties remains feasible in such cases. To illustrate the main idea of the two-step control algorithm we restrict ourselves to the minimal model. We consider the stabilization of a simple fixed point that does not require the use of the unstable controller and apply the simple DFC algorithm (not the extended version).

To be specific, we demonstrate our approach for the logistic map $x_{n+1}=f(x_n;a)$, where $f(x_n;a)=ax_n(1-x_n)$. The map has a period-1 orbit $x^*=1-1/a$, which is unstable for $a>3$. Our aim is to stabilize it via the two-step DFC algorithm. We suppose that a is an accessible control parameter. When increasing this parameter the system undergoes the period-doubling bifurcation and reaches a chaotic regime. The key idea of applying the two-step control to this system is as follows. In the first step, we shift the parameter to the interval $1<a<3$, where the period-1 orbit is stable, and thus generate an extraneous orbit. In the second step, we return the original value of the parameter a and switch on the DFC algorithm in order to stabilize the target orbit. In other words, we adjust the control parameter a on each iteration by an amount $-(1-C)\Delta a+Ck(x_n-x_{n-1})$ such that the controlled system is described by a two-dimensional map

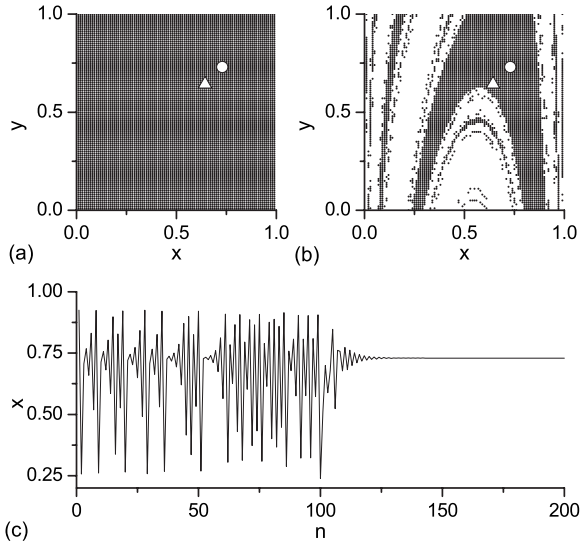

FIG. 6. Basins of attraction of (a) extraneus orbit ($C=0$) and (b) target orbit ($C=1$, $k=2$) for $a=3.7$ and $\Delta a=0.9$. Extraneous and target orbits are shown, respectively, by triangles and circles. In (c) the dynamics of the two-step control is demonstrated. For $n<100$ the control is off ($C=1$, $k=0$). The first step ($C=0$) lasts five iterations in the time interval $100\leqslant n\leqslant 104$. The second step ($C=1$, $k=2$) is activated for $n\geqslant 105$.

$$x_{n+1}=[a-(1-C)\Delta a+Ck(x_n-y_n)]x_n(1-x_n),$$

$$y_{n+1}=x_n. \tag{A1}$$

For $C=1$ and $k=0$, we have the free logistic map. In the first step, we take $C=0$, such that the parameter a is decreased by an amount Δa. As a result there appears an extraneous orbit $x_e=1-1/(a-\Delta a)$ with Floquet multiplier $\mu_e=2-a+\Delta a$. If $1<a-\Delta a<3$, the extraneous orbit is stable and the system approaches it during the characteristic time $\tau_e=1/|\ln|\mu_e||$. Thus the duration t_C of the first step should satisfy $t_C>\tau_e$. In the second step, we return the original value of the parameter a by switching on $C=1$ and activate the DFC control by switching on $k\neq 0$. The linear analysis of the system (A1) at $C=1$ shows that the target orbit $(x,y)=(x^*,x^*)$ is stable if the control gain is in the interval

$$\frac{a-3}{2}\frac{a^2}{a-1} < k < \frac{a^2}{a-1}. \tag{A2}$$

In Fig. 6 we demonstrate the numerical results for the parameters $a=3.7$ and $\Delta a=0.9$. We see that the basin of attraction of the extraneous orbit occupies the whole unity square $0<x<1$, $0<y<1$. The characteristic time of approaching this orbit is $\tau_e \approx 4.48$. The basin of attraction of the target orbit is shown in Fig. 6(b). It occupies only about 45% of the unity square. Thus the usual one-step DFC algorithm is successful only for 45% of initial conditions taken from the unity square. In contrast, the two-step control ensures 100% success for any initial conditions taken from the unity square. This is provided by two features of the extraneous orbit: (i) the extraneous orbit lies in the basin of attraction of the target orbit and (ii) the basin of attraction of the extraneous orbit occupies the whole unity square. In Fig. 6(c) we show the dynamics of the system controlled by the two-step algorithm when the duration of the first step $t_C=5$ only slightly exceeds the characteristic time τ_e.

[1] *Handbook of Chaos Control*, edited by H. G. Schuster (Wiley-VCH, Berlin, 1999).
[2] S. Boccaletti, C. Grebogi, Y. C. Lai, H. Mancini, and D. Maza, Phys. Rep. **329**, 103 (2000).
[3] D. J. Gauthier, Am. J. Phys. **71**, 750 (2003).
[4] E. Ott, C. Grebogi, and J. A. Yorke, Phys. Rev. Lett. **64**, 1196 (1990).
[5] K. Pyragas, Phys. Lett. A **170**, 421 (1992).
[6] J. E. S. Socolar, D. W. Sukow, and D. J. Gauthier, Phys. Rev. E **50**, 3245 (1994).
[7] A. Kittel, J. Parisi, and K. Pyragas, Phys. Lett. A **198**, 433 (1995).
[8] Th. Mausbach, Th. Klinger, A. Piel, A. Atipo, Th. Pierre, and G. Bonhomme, Phys. Lett. A **228**, 373 (1997).
[9] A. Ahlborn and U. Parlitz, Phys. Rev. Lett. **93**, 264101 (2004).
[10] K. Pyragas, Philos. Trans. R. Soc. London, Ser. A **364**, 2309 (2006).
[11] W. Just, T. Bernard, M. Ostheimer, E. Reibold, and H. Benner, Phys. Rev. Lett. **78**, 203 (1997).
[12] H. Nakajima, Phys. Lett. A **232**, 207 (1997).
[13] H. Nakajima and Y. Ueda, Physica D **111**, 143 (1998).
[14] B. Fiedler, V. Flunkert, M. Georgi, P. Hövel, and E. Schöll, Phys. Rev. Lett. **98**, 114101 (2007).
[15] K. Pyragas, Phys. Rev. Lett. **86**, 2265 (2001).
[16] K. Pyragas, V. Pyragas, and H. Benner, Phys. Rev. E **70**, 056222 (2004); V. Pyragas and K. Pyragas, *ibid.* **73**, 036215 (2006).
[17] K. Höhne, H. Shirahama, C.-U. Choe, H. Benner, K. Pyragas, and W. Just, Phys. Rev. Lett. **98**, 214102 (2007).
[18] C. von Loewenich, H. Benner, and W. Just, Phys. Rev. Lett. **93**, 174101 (2004).
[19] W. Just, H. Benner, and C. Loewenich, Physica D **199**, 33 (2004).
[20] K. Yamasue and T. Hikihara, Phys. Rev. E **69**, 056209 (2004).
[21] P. Cvitanović, Phys. Rev. Lett. **61**, 2729 (1988).
[22] A. Kittel, K. Pyragas, and R. Richter, Phys. Rev. E **50**, 262 (1994).
[23] Y.-Ch. Lai, A. Kandangath, S. Krishnamoorthy, J. A. Gaudet, and A. P. S. de Moura, Phys. Rev. Lett. **94**, 214101 (2005).
[24] A. Namajunas, K. Pyragas, and A. Tamaševičius, Phys. Lett. A **201**, 42 (1995).